ORIGINAL PAPER

Electrochemical sensing of lactate by using an electrode modified with molecularly imprinted polymers, reduced graphene oxide and gold nanoparticles

Thulio César Pereira [1,2] · Nelson Ramos Stradiotto [1,2]

Abstract

This paper reports on a sensitive and selective electrochemical sensor for lactic acid. The sensor is based on molecularly imprinted polymers (MIP), obtained on glassy carbon electrode (GCE) modified with reduced graphene oxide and gold nanoparticles. The MIP was obtained by electropolymerization of the o-phenylenediamine (o-PD) on the modified surface of the GCE in the presence of lactic acid. The steps involving the GCE modification and MIP construction were characterized by cyclic voltammetry, electrochemical impedance spectroscopy, scanning electron microscopy and atomic force microscopy. The results were evaluated using differential pulse voltammetry, using the hexacyanoferrate redox system as an electrochemical probe. Under optimized experimental conditions, the imprinted sensor has a linear response in the 0.1 nM to 1.0 nM lactic acid concentration range, with detection limit of 0.09 nM. The sensor exhibits excellent selectivity in the presence of molecules of similar chemical structure. It was applied for the selective determination of lactic acid in sugarcane vinasse. The recovery values ranged from 97.7 to 104.8%.

Keywords Lactic acid · Electrochemical sensor · Sugarcane vinasse · Electropolymerization · o-Phenylenediamine

Introduction

Lactic acid is an antioxidant, acidulate and humectant [1], which make it suitable for application in diverse areas, including the food, chemical, biochemical, medical, cosmetics and pharmaceutical industries [2–4]. In addition, lactic acid can be used as raw material for the large-scale production of biodegradable polymers which can substitute conventional plastic materials [5, 6]. Lactic acid

monitoring plays an essentially vital role in various fields. The compound is often used as an indicator for the presence of bacteria in food, and thus can be used to determine the quality of food. Furthermore, the concentration of lactic acid in the blood can be used for monitoring respiratory insufficiency, heart failure and shocks [7, 8].

Many analytical methods for the determination of organic acids have been reported in the literature, among the main ones employed include those based on Gas Chromatography (GC), Capillary Electrophoresis (EC) and High Performance Liquid Chromatography (HPLC). Although these techniques are found to be efficient for the detection and determination of organic acids, they often present some non-negligible shortcomings, such as appropriate samples preparation, including clean up and/or sample derivatization and the requirement for employing well trained professionals to operate the equipment [9–15].

In this sense, a simple, sensitive and selective method for lactic acid detection is desirable and useful for the performance of routine analytical practice. Electrochemical sensors

✉ Thulio César Pereira
tuliocs22@gmail.com

1 Institute of Chemistry, São Paulo State University (UNESP), Araraquara, São Paulo CEP:14800-060, Brazil

2 Bioenergy Research Institute, São Paulo State University (UNESP), Araraquara, São Paulo CEP:14800-060, Brazil

exhibit high sensitivity, and involve low costs and relatively shorter time of analyses compared to other analytical methods. Remarkably, very few works have been published in the literature regarding the application of electrochemical detection for lactic acids [4, 7, 8, 16–22]. Among the electrochemical methods reported in the literature, the method involving the use of amperometric biosensors using the enzyme lactate oxidase are considered the fastest, simplest and most selective method for lactic acid monitoring. However, the unstable nature of the enzymes (recognition agents) is regarded the main demerit concerning the use of biosensors, especially when working with complex and low pH samples, such as sugarcane vinasse.

Electrochemical sensors based on molecularly imprinted polymers (MIP) have drawn considerable interests in the last few years due to the fact that the molecularly imprinted technique provides the sensor with higher selectivity, in addition to greater reliability and stability (mechanical and chemical). The molecular imprinted process involves the polymerization of suitable functional monomers in the presence of a template molecule (usually the analyte) and the subsequent extraction of the template from the polymer network with the aid of a solvent. This procedure generates selective cavities, which are capable of recognizing the analyte through a rebinding process in any matrices of interest without interference [23].

The electropolymerization technique has become the most widely employed technique for the development of electrochemical sensors based on MIP; the reason being that, in comparison to other techniques, this method presents far more advantages. Among these advantages includes the control of thickness of the electrodeposited film and its morphology through electropolymerization conditions (e. g. number of cyclic scan, applied voltage), apart from the fact that the method allows better adhesion of the polymeric film on the electrode [24–26].

To date, only one article has been published in the literature which sought to demonstrate the construction and application of electrochemical sensors based on MIP for the determination of lactic acid [27]. Although it shows a rapid response, the method applied for the production of MIP (chemical polymerization) may impair the analytical performance of the sensor due to problems related to mass transport, lack of accessibility to imprinting sites, agglomeration of cavities, and slow kinetics.

The present work proposes the construction of electrochemical sensor based on MIP obtained through the electropolymerization of o-PD monomer on a modified surface with RGO and AuNPs for the determination of lactic acid. The proposed sensor benefits from the electrical properties of AuNPs, which help to provide a better electrochemical response for the probe, and the high surface area of RGO,

which can help to prevent AuNPs agglomeration. The combination of these materials with MIP allows one to obtain an electrochemical sensor with superior analytical performance.

Experimental

Reagents and apparatus

All the solutions were prepared with ultrapure water. Lactic acid (purity ≥98%), o-phenylenediamine (purity: ≥ 98%), potassium ferricyanide ($K_3[Fe(CN)_6]$, purity: ≥ 99%), potassium ferrocyanide ($K_4[Fe(CN)_6]$ purity ≥99%), graphene oxide suspension (purity: > 95%), chloroauric acid ($HAuCl_4$) were purchased from Sigma-Aldrich (https://www.sigmaaldrich.com). Potassium chloride (KCl), potassium hydrogen phosphate, and dipotassium hydrogen phosphate were used as supporting electrolyte and for the preparation of buffer, respectively. Acetonitrile (ACTN) was used to extract the template molecule from the polymer matrix. Stock solution of 5.0×10^{-2} mol L^{-1} lactic acid and o-phenylenediamine were prepared in 0.1 mol L^{-1} phosphate buffer (PB) under pH 5.0 for electropolymerization. For rebinding, PB (0.1 mol L^{-1}) of pH 6.0 was used. The electrochemical active probe solution applied was 5.0×10^{-3} mol L^{-1} in 0.1 mol L^{-1} of KCl.

The electrochemical measurements were performed using potentiostat Autolab PGSTAT30 coupled to a microcomputer which records data obtained using the control software Nova 1.11. A conventional three-electrode system was employed; this consisted of glassy carbon electrode (3.0 mm in diameter) used as working electrode, Ag/AgCl (KCl 3.0 mol L^{-1}) employed as reference electrode, and platinum wire as auxiliary electrode. All experiments were carried out at room temperature.

Cleaning the glassy carbon electrode (GCE)

The GCE was polished with 0.30 μm alumina powder on a felt and electrochemically polished by successive scans at potential range of −0.50 to +1.50 V in 0.50 mol L^{-1} H_2SO_4 at 50 mV s^{-1} until cyclic voltammogram characteristics of a cleaned GCE were obtained. Thereafter, the electrode was sonicated for 2 min in deionized water.

Preparation of the AuNP/RGO/GCE

The reduced graphene oxide (RGO) film was electrodeposited on GCE as reported in previous works by our research group [28, 29]. Briefly, 0.50 mg mL^{-1} of graphene oxide (GO) suspension was dispersed in 0.10 mol L^{-1} Na_2SO_4 used as supporting electrolyte. The film was deposited by applying a potential of −1.5 V for 600 s. using chronoamperometry. The electrode was then dried at room temperature.

The AuNPs were electrodeposited onto the RGO in solution containing 5.0×10^{-4} mol L^{-1} HAuCl$_4$ in 0.50 mol L^{-1} H$_2$SO$_4$. The potential applied for the electrodeposition process was +0.50 V for 100 s. This process was employed because it allows the control of the RGO film thickness and the size of the deposited AuNPs with excellent reproducibility and good stability.

Preparation of imprint

The MIP was prepared by electropolymerization using CV in the range of 0.0 V to 0.8 V at 50 mV s^{-1} for 25 consecutive cycles in 0.10 mol L^{-1} PB under pH 5.0 containing 1.0×10^{-3} mol L^{-1} o-PD as functional monomer and 2.0×10^{-4} mol L^{-1} lactic acid as template. After undergoing electropolymerization, the MIP modified electrode was denominated MIP/AuNP/RGO/GCE. Following electropolymerization, the electrode was soaked in PB solution of pH 5.0 aiming at removing non-polymeric monomers on the electrode surface. Subsequently, the MIP/AuNP/RGO/GCE was immersed in acetonitrile (ACTN) for 60 s at room temperature under stirring in order to extract the embedded lactic acid and form imprinted cavities. The cavities exhibit strategically positioned functional groups which are capable of interacting with the functional group of the lactic acid. In addition, the cavities have shape and size similar to the acid molecule; and this allows for a selective rebinding process. For the purposes of comparison and control, a non-imprinted polymer electrode, named NIP/AuNPs/RGO/GCE, was constructed based on the same procedure employed toward constructing the MIP modified electrode. Unlike the MIP modified electrode, the non-imprinted polymer electrode was constructed without the presence of lactic acid in order to evaluate the reliability of the measurements.

Electrochemical measurements

After the extraction step, the modified GCE was subjected to rebinding experiments. The rebinding of lactic acid in the cavities formed in the polymer was performed through the immersion of the MIP/AuNPs/RGO/GCE electrode in different concentrations of lactic acid solution in 10 mL of 0.10 mol L^{-1} PB (pH 6.0) under stirring for 10 min. After that, the electrode was subsequently placed in a three electrode conventional cell with the MIP/AuNPs/RGO/GCE acting as the working electrode. The redox pair [Fe(CN)$_6$]$^{3-/4-}$ was chosen as electrochemical active probe in order to study the performance of the sensor. A solution of 0.10 mol L^{-1} KCl containing 5.0×10^{-3} mol L^{-1} [Fe(CN)$_6$]$^{-3/-4}$ was used to conduct the study .

The analytical data were obtained using DPV technique based on the peak current variation of the probe [Fe(CN)$_6$]$^{3-/4-}$. To this end, the current shift (ΔI) was calculated taking into account the oxidation peak currents of the probe after removing the lactic acid molecules with ACTN and following the rebinding of the lactic acid molecules in the cavities generated after 10 min of contact.

The figures of merit: limit of quantification (LOQ), limit of detection (LOD) and amperometric sensitivity (As), were calculated. LOQ and LOD according to the equation LOQ = 10 SD/S and LOD = 3.3 SD/S, where SD is the standard deviation of the intercept, and S is the slope of the calibration plot.

After the electrodeposition of RGO and AuNPs and the construction of the MIP, electrochemical impedance spectroscopy (EIS) was employed in order to characterize the electronic transfer properties of the sensor. The EIS was carried out at a potential of 0.22 V over the frequency range of 5 mHz to 100 kHz and amplitude rms of 10 mV. In addition to the EIS, cyclic voltammetry analysis was also employed as part of the electrochemical characterization.

Scanning electron microscopy with field emission gun (SEM-FEG) was employed aiming at studying the morphology of the surface after the electrodeposition of RGO and AuNPs along with the formation of the MIP. Furthermore, atomic force microscopy (AFM) was also used to characterize the modified surface in the stages of electropolymerization, removal and rebinding during the construction of the MIP.

Determination of lactic acid in sugarcane vinasse sample

The sugarcane vinasse samples were centrifuged at 4000 rpm for 25 min in order to remove the solid particles. The supernatant was collected and filtered using filters of 0.47 and 0.22 μm porosity. Subsequently, 5.0 μL of the filtered vinasse were diluted in 50 mL of PB solution under pH 6.0. For the analyte determination in sugarcane vinasse, lactic acid concentrations ranging from 4.0×10^{-10} mol L^{-1} to 8.0×10^{-10} mol L^{-1} were added to the samples by the standard addition method. Recovery tests were performed by adding a defined concentration of lactic acid in the sugarcane vinasse samples.

Results and discussion

Preparation of the molecularly imprinted polymer (MIP)

Among the various monomers available for the construction of MIP, o-phenylenediamine has become increasingly prominent in recent years, being widely used for the construction of electrochemical sensors. The growing popularity of this monomer lies, mainly, in the fact that it allows the production of thin and compact films on the electrode surface, which improves the sensor response.

Some MIP-based electrochemical sensors may suffer from low conductivity, depending mainly on the nature of the

polymeric film and its thickness. Often, in the search for a larger number of selective sites, a very thick polymer is obtained; this makes the probe difficult to reach to the electrode surface in order to obtain the signal. To overcome these problems, new MIPs have been constructed on nanostructured surfaces, which offer a larger number of locations for the molecular printing process. Among these nanomaterials, gold nanoparticles have drawn considerable interest. The reason being that gold nanoparticles are found to offer other advantages when it comes to the construction of electrochemical sensors. Among these additional advantages include excellent electrical conductivity and good compatibility with a wide range of polymers.

The cyclic voltammogram recorded during the electropolymerization of o-PD monomer in the presence of lactic acid on the glassy carbon electrode (GCE) modified with reduced graphene oxide (RGO) and gold nanoparticles (AuNPs) are shown in Fig. S1.

In the first scan cycle, one notices the oxidation peak of o-PD monomer at 0.43 V, the radical cation formed in this step is responsible for triggering and maintaining the polymerization reaction. The results obtained show that the process is completely irreversible. In the second scan cycle, one will observe that the peak current decreases progressively with each cycle, tending to zero. This behavior confirms the formation of a compact and poorly conductive polymer layer on the modified surface of the electrode.

The molecular imprinted process is shown in Fig. 1, where one can observe the possible formation of hydrogen bonds between the hydrogen of the N-H groups present in the o-PD monomer and the carboxyl and hydroxyl groups of lactic acid (pK_a = 3,9). These interactions are mainly responsible for the process of rebinding of lactic acid (in the form of lactate) in the imprinted cavities of the MIP, allowing its recognition in a complex matrix.

Electrochemical characterization of MIP/AuNP/RGO/GCE

For each step involving the GCE modification in the sensor construction, electrochemical characterization was performed by CV and EIS analyses using 0.10 mol L^{-1} KCl containing 5.0×10^{-3} mol L^{-1} $[Fe(CN)_6]^{-3/-4}$. All CV experiments were performed at a scan rate of 50 mV s^{-1}. The cyclic voltammograms obtained for the first step involving GCE modification with RGO and AuNPs are shown in Fig. S2.

The typical of pair of redox peaks related to the probe can be observed on the bare GCE electrode (curve a). After the modification of the GCE with RGO, a sharp increase is observed in the peak current (curve b). The increase in peak current is attributed to the increase in both the electrical conductivity and the surface-to-volume ratio triggered by the electrodeposited RGO on the GCE surface.

When the RGO/GCE electrode is modified with gold nanoparticles, a considerable increase in current is observed again (curve c). This behavior is associated with the increase in the surface area of the electrode and in the size of the electrodeposited nanoparticles, which facilitates the occurrence of electronic transfer.

The EIS analysis was also used to characterize the interface properties of the modified electrode in terms of charge transfer resistance (R_{ct}), which is calculated using the diameter of the semicircle in the Nyquist diagram.

The Nyquist diagram obtained for different steps involving the modification of the electrode surface are shown in Fig. S3. One will clearly observe that the value of R_{ct} decreases progressively when the GCE electrode R_{ct} = 710.3 Ω (curve a) is first modified with RGO R_{ct} = 520.7 Ω (curve b) and subsequently with AuNPs R_{ct} = 290.7 Ω (curve c). This behavior confirms that the redox process for the $[Fe(CN)_6]^{-3/-4}$ species is facilitated when the modifications are performed on the electrode surface.

The equivalent electrical circuit, which best represents the experimental data obtained, is shown in the inset of Fig. S3. The circuit is formed by a resistance (R_s), which is related to the solution resistance, connected, in series, to the arrangement formed by a constant phase element (CPE); the CPE is related to the double layer capacitance, which is connected in parallel to a second resistance (R_{ct}) - the charge transfer resistance. The charge transfer resistance is connected in series to the Warburg element (W), which indicates that the redox process on the electrode surface is controlled by diffusion.

After the modification of the electrode surface, the electropolymerization of o-PD monomer was carried out with the aim of constructing the MIP and the NIP electrode. The cyclic voltammograms obtained for each of the stages involving the construction of the MIP sensor are shown in Fig. 2A. After electropolymerization, no redox peaks are observed for the MIP (curve a) and NIP (curve d). The behavior observed here suggests the formation of a compact and poorly conductive film on the surface of the modified electrode; this inhibits the electronic transfer of the probe, thus confirming the success of the electropolymerization step.

After the extraction of lactic acid molecules, using acetonitrile as solvent, the redox peaks for the species $[Fe(CN)_6]^{-3/-4}$ can be visualized again (curve b). This confirms the formation of imprinted cavities in the MIP, which facilitates the electronic transfer of the probe. When the modified GCE is placed in 0.1 mol. L^{-1} PB (pH 6.0) containing a solution of 5.0×10^{-10} mol L^{-1} of lactic acid for 10 min, one notices a significant decrease in the peak current (curve c). This indicates that some imprinted cavities obtained in the previous step were again occupied by lactic acid in a rebinding step, making it difficult the electronic transfer of the probe.

The preparation steps of the MIP were also studied using the EIS technique; the results obtained with the aid of the
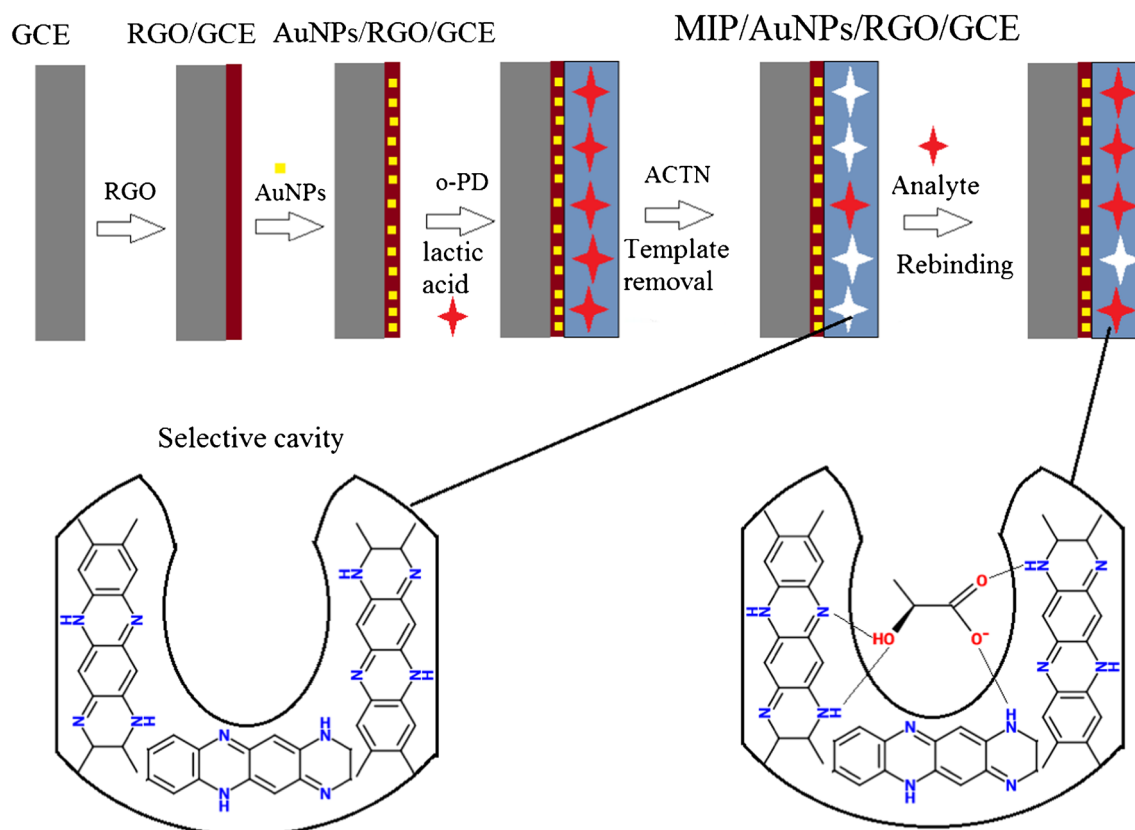
Fig. 1 Schematic representation of molecular imprinting of lactic acid using o-PD as functional monomer

Nyquist diagram are shown in Fig. 2B. When one observes the Nyquist diagram after polymerization (curve a), one notices the presence of a new resistance; in other words, one observes the presence of a new intercept on the real impedance axis (Z' axis) in the region of high frequencies, which is confirmed by the inset in Fig. 2B.

The new resistance observed in the Nyquist diagram was associated with the (polymer matrix) film diffusional resistance (R_f), which make difficult the electronic transfer. This behavior is confirmed by the increase in R_{ct} value. After polymerization, the R_{ct} value obtained was 44.1 kΩ (curve a); this result confirms the compact and non-conductive nature of the polymeric film obtained on the electrode surface, which makes it difficult for the probe to reach the electrode surface.

Upon the removal of the lactic acid molecules from the polymer matrix, a decrease is observed in the $R_{ct} = 8.3$ kΩ values (curve b), suggesting that the imprinted cavities have been successfully obtained and the probe can reach the electrode surface more easily. The value of R_{ct} (23.7 kΩ) increases again (curve c) after the rebinding step; this is attributed to the fact some imprinted cavities are once again occupied by the lactic acid, making it difficult for the probe to reach the surface of the electrode.

As performed in the first step involving the electrode modification, the results obtained in the preparation of MIP were

also interpreted in terms of equivalent electrical circuit (inset of Fig. 2B). The best fit circuit for the data consists of two arrangements, similar to the circuit obtained for, which is composed of the following elements: R_s, CPE, R_{ct} and W (the same as the previous step of electrode modification). These elements are connected in series with a parallel arrangement of those elements related to the polymer film on the electrode surface, a new CPE_f - which is related to interfacial capacitance of the film, and a new resistor R_f - which is related to the film diffusional resistance imposed on the probe inside the polymer film [30, 31].

In order to verify some preliminary results obtained via the EIS technique, studies were conducted using the CV technique to confirm the nature of the electrode process on the electrode surface for the probe after the removal of the template molecule. As can be seen in Fig. S4, the anodic (I_{pa}) and cathodic (I_{pc}) peak currents on the imprinted electrode were found to increase with an increase in scan rate ranging from 25 to 250 mV s^{-1}; here, the values of I_{pa} and I_{pc} are seen to vary linearly with the root square of scan rate. The I_{pa} and I_{pc} showed a linear dependence with the root speed ($v^{1/2}$), which can be expressed as: I_{pa} (μA) $= 2.7 \times 10^{-6} v^{1/2} + 8.3 \times 10^{-6}$ (R2 = 0.998) and I_{pc} (μA) $= -2.7 \times 10^{-6} v^{1/2} - 8.7 \times 10^{-6}$ (R2 = 0.998). This behavior indicates that the proposed electrochemical sensor has a diffusion-controlled redox process for the [Fe(CN)$_6$]$^{-3/-4}$ species used as probe, thus confirming
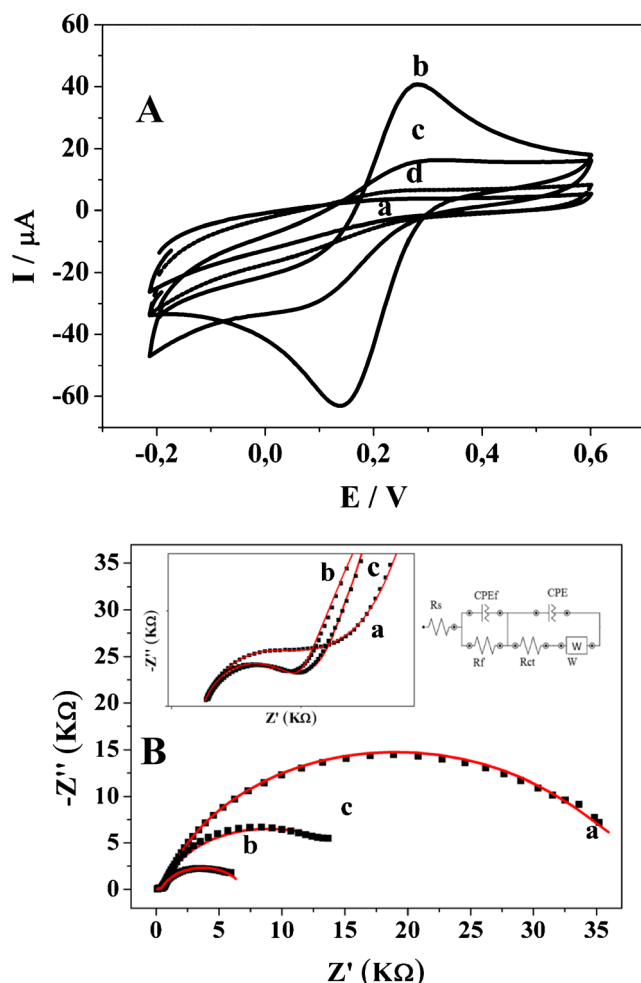
Fig. 2 (A) Cyclic voltammograms, at scan rate of 50 mV s^{-1}, for: (a) MIP/AuNP/RGO/GCE after electropolymerization (b) MIP/AuNP/RGO/GCE after template removal and (c) MIP/AuNP/RGO/GCE after lactic acid rebinding (d) NIP/AuNP/RGO/GCE. (B) Nyquist diagrams for (a) MIP/AuNPs/RGO/GCE after electropolymerization (b) MIP/AuNPs/RGO/GCE after template removal and (c) MIP/AuNP/RGO/GCE after lactic acid rebinding in solution containing 5.0×10^{-3} mol L^{-1} [Fe(CN)$_6$]$^{3-/4-}$ in 0.10 mol L^{-1} KCl. The frequency range in EIS was from 5 mHz to 100 kHz

the preliminary results obtained through the EIS technique. Essentially, the results show an ideal behavior required of an electrochemical sensor.

Surface morphological characterization of the imprint

Figure S5a shows the SEM images of RGO/GCE, by observing the images, one will notice the characteristic wrinkled appearance of electrodeposited graphene nanosheets. This characteristic graphene arrangement is responsible for the increased surface area of the electrode. Fig. S5b shows the image of a uniform electrodeposition of AuNPs on graphene nanosheets with homogeneous distribution on the RGO/GCE; this image indicates the success of the deposition of gold nanoparticles

on the RGO/GCE surface. As can be seen in Figs. S5c and S5d, the electropolymerization process was successfully performed for MIP/AuNPs/RGO/GCE and NIP/AuNPs/RGO/GCE, respectively, covering the AuNPs electrodeposited on the graphene nanosheets. The EDX spectrum is shown in Fig. S5e; it confirms the presence of gold on the electrode surface (the electrode surface presented an average diameter of 90 ± 15 nm, see Fig. S5f). The AFM 3D images for each of the steps involving the MIP construction are shown in Fig. 3. One can observe the homogeneous modification on the electrode surface after electropolymerization of the monomer for MIP/AuNPs/RGO/GCE.

The AFM 3D images obtained were analyzed in terms of roughness of the electrode surface after each step involving the construction of the MIP. The results were evaluated in terms of the root-mean-square (RMS) value, which is proportional to the roughness of the surface. For the MIP/AuNP/RGO/GCE and NIP/AuNP/RGO/GCE electrodes, the values obtained were 43.9 nm and 31.4 nm (Fig. 3a and d), respectively. After the removal of the template using acetonitrile as solvent (see Fig. 3b), a significant change was observed in the RMS value - the value obtained was 64.9 nm. This increase in RMS value is attributed to the changes provoked by the solvent in the polymer structure, which allowed the removal of the lactic acid molecules, thus forming cavities in the polymer matrix. After rebinding (see Fig. 3c), the RMS value obtained was 51.7 nm. This decrease in RMS value may be related to the occupation of some cavities formed in the previous stage.

Optimization of conditions for MIP preparation

The nature of monomer, the ratio of monomer to template, the pH and the number of CV scan cycle during the electropolymerization, removal time and rebinding time are key factors that tend to influence the performance of the MIP modified sensor. All these parameters allow one to obtain a polymer with adequate thickness and good physical stability on the electrode surface, thus paving the way toward obtaining selective cavities capable of recognizing the analyte. In view of that, these factors were studied and optimized in order to achieve the best experimental conditions for the development and application of the MIP. Discussions on each of the optimized parameters can be found in the Supplementary Material section.

All the experiments related to the optimization step were performed using the DPV technique. In addition, changes in the current (ΔI) related to the oxidation of the probe after the removal of template and after rebinding were taken into account so as to evaluate the optimum condition for each parameter.

In summary, the experimental conditions optimized to obtain the MIP were as follow: electropolymerization performed

Fig. 3 AFM images: (a) MIP/AuNP/RGO/GCE before the removal of template (b) MIP/AuNP/RGO/GCE after the removal of template (c) MIP/AuNPs/RGO/GCE after rebinding and (d) NIP/AuNP/RGO/GCE
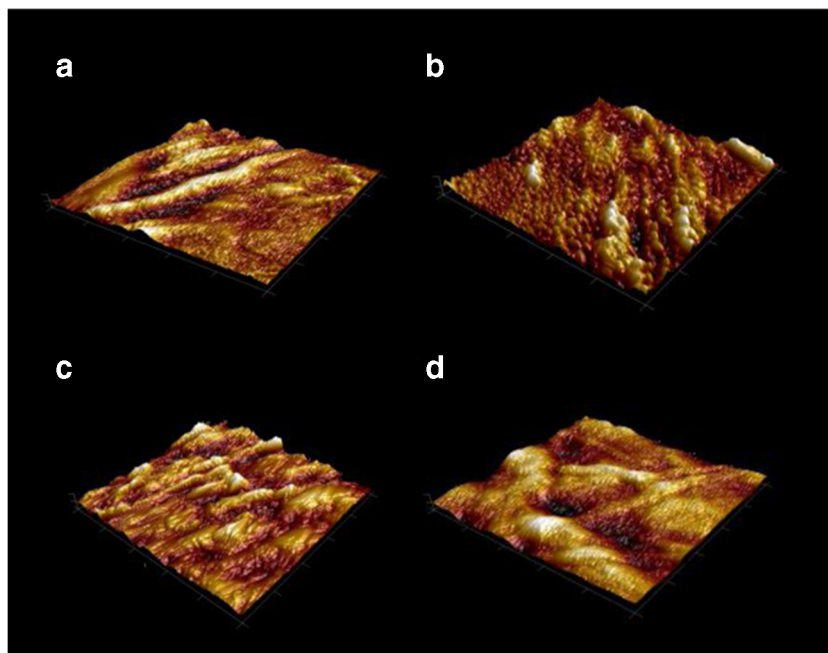
in the potential range of 0.0 V to 0.8 V for 25 cycles in PB solution at pH 5.0, using o-PD as functional monomer (at a concentration of 1.0×10^{-3} mol L^{-1}) and lactic acid as template (at a concentration of 2.0×10^{-4} mol L^{-1}).

Analytical performance

After optimization, preparation and characterization of the MIP/AuNP/RGO/GCE, the analytical curve was obtained using the DPV technique after rebinding of different concentrations of lactic acid. The analytical curve obtained is shown in Fig. 4.

To obtain the analytical curve, after the extraction of the template, the sensor was subjected to successive rebinding processes using solutions containing different concentrations of lactic acid (from 1.0×10^{-10} mol L^{-1} to 1.5×10^{-8} mol L^{-1}) for 10 min. At the conclusion of the rebinding step for lactic acid, the peak current was measured for the electrochemical probe oxidation.

The peak current for probe oxidation was found to decrease with an increase in lactic acid concentration (DPV - inset Fig. 4). This may be attributed to the fact that the MIP cavities are being progressively occupied by the lactic acid molecules, which makes it difficult to diffuse the probe inside the polymer matrix to the electronic transfer on the electrode.

Figure 4 shows that the current response for the probe oxidation is proportional to the concentration of lactic acid in two different concentration ranges: from 1.0×10^{-10} to 1.0×10^{-9} mol L^{-1} and from 2.0×10^{-9} to 1.5×10^{-8} mol L^{-1}. The first linear range was used to calculate the figures of merit. The linear regression equation obtained was: $\Delta I \, (\mu A) = 1.9 \times 10^5 \, C_{Lactic \, acid} + 1.4 \times 10^{-5}$ with a correlation

coefficient of 0.998, LOD = 8.9×10^{-11} mol L^{-1}, LOQ = 1.9×10^{-10} mol L^{-1}, and amperometric sensitivity (As) of 1.9×10^5 μA L mol^{-1}.

Table 1 shows the results obtained for the MIP/AuNP/RGO/GCE in comparison with other methods reported in the literature for lactic acid detection. The method proposed in this work exhibited relatively lower detection and
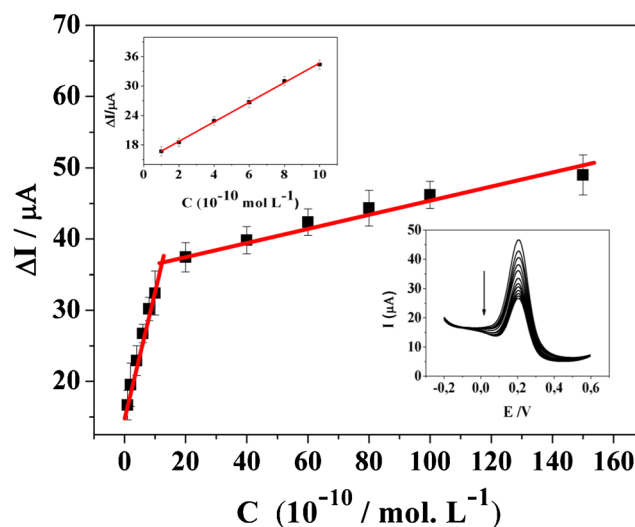
Fig. 4 Calibration curve for lactic acid detection using the MIP/AuNP/RGO/GCE in different lactic acid concentrations (from 1.0×10^{-10} mol L^{-1} to 1.5×10^{-8} mol L^{-1}) in PB solution of pH 6.0, after 10 min of rebinding, using 5.0×10^{-3} mol L^{-1} [Fe(CN)$_6$]$^{3-/4-}$ as probe. The inset on the upper left corresponds to the curve obtained in the lactic acid concentration ranging from 1.0×10^{-10} mol L^{-1} to 1.0×10^{-9} mol L^{-1}. The inset at the bottom corresponds to the DPV obtained after each rebinding step

Table 1 Comparison of linear range and detection limits of the method proposed in this study with those reported in the literature for the determination of lactic acid

Detection method	Linear range (mol L^{-1})	Detection limit (mol L^{-1})	Reference
Gold electrode	5.0×10^{-6} – 340×10^{-6}	0.96×10^{-6}	[7]
NiO and Ni(OH)	1.0×10^{-5} – 3.27×10^{-2}	5.3×10^{-4}	[16]
ZnO nanorods	1.0×10^{-7} – 1.0×10^{-3}	1.0×10^{-7}	[17]
MIP/MWCNTs/PVC	1.0×10^{-6} – 1.0×10^{-1}	7.3×10^{-7}	[23]
Nafion/Lox/ (PPy-F127)/GCE	1.5×10^{-5} – 3.75×10^{-5}	8.8×10^{-6}	[30]
MIP/AuNPs/ RGO/GCE	1.0×10^{-10} – 1.5×10^{-8}	8.93×10^{-11}	This work

Fig. 5 Rebinding isotherm for MIP/AuNP/RGO/GCE electrode

quantification limits compared with the methods reported in the literature.

Rebinding study

The existence of two linear concentration ranges is related to the presence of selective recognition sites in the MIP with different affinities for the analyte molecules. When the lactic acid concentration is lower, the molecules tend to occupy the cavities with more affinity, located at the upper region of the polymeric film.
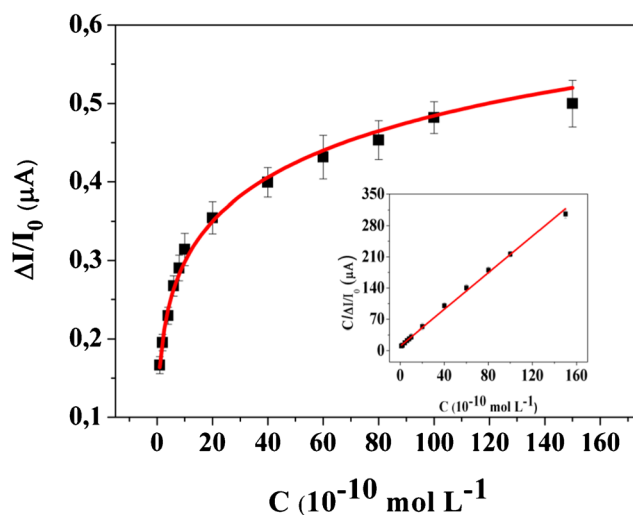
Inversely, the sites with the lowest affinity located inside the film are occupied only when all the sites with higher affinity are already occupied, i.e. when the lactic acid concentration is increased. This condition leads to a decrease in the sensor response, and consequently triggers a decline in the slope of the line to the second linear range.

Based on the existence of these two types of binding sites in the MIP, a binding isotherm (Fig. 5) was obtained with the aim of evaluating the analyte interaction in the MIP cavities. The calculation was done based on eq. 01 below [32, 33].

$$\frac{\Delta I}{I_0} = \frac{B_{max} \, C}{K_d + C} + NsC \quad (1)$$

Where C is the bulk concentration of analyte, B_{max} is the maximum number of binding sites in the MIP, K_d being equilibrium dissociation constant, and Ns representing the binding constant for non-specific adsorption. The value of Kd obtained with the fitting was 4.9×10^{-7} mol L^{-1} (R = 0,997); this implies that the lactic acid exhibited a high affinity for the MIP recognition sites.

To evaluate the sensor stability, the imprinted sensor was stored at room temperature (25 °C) for 21 days after template removal and rebinding. At the end of this period, the electrode still displayed 89.7% of the initial current, with *RSD* of 3.2%. These results indicate that the electrode (modified with RGO, AuNPs and MIP) proposed in this work presents good stability.

Selectivity of the MIP/AuNPs/RGO/GCE

The selectivity of the MIP/AuNP/RGO/GCE was studied by comparing the DPV response (ΔI) for probe oxidation after rebinding of lactic acid and the response for probe oxidation after rebinding of some molecules found in sugarcane vinasse that can act as interferents. For each of the molecules, the electrodes were constructed under optimized conditions. For the rebinding process, 10 nM solutions were used for each of the interferents.

Figure 6 shows the current intensity response for the probe oxidation after 10 min contact of the MIP for the rebinding of lactic acid and the rebinding of possible interferents under investigation. Here, one notices that the response relative to lactic acid is considerably higher compared to the response related to the interferents; this confirms that the sensor has excellent selectivity for the analyte detection.

To evaluate the specificity and selectivity of the MIP/AuNPs/RGO/GCE, the imprinting factor (α) and selectivity factor (β) were calculated according to eqs. 02 and 03 below:

$$\alpha = \frac{\Delta I \, (MIP)}{\Delta I \, (NIP)} \quad (2)$$

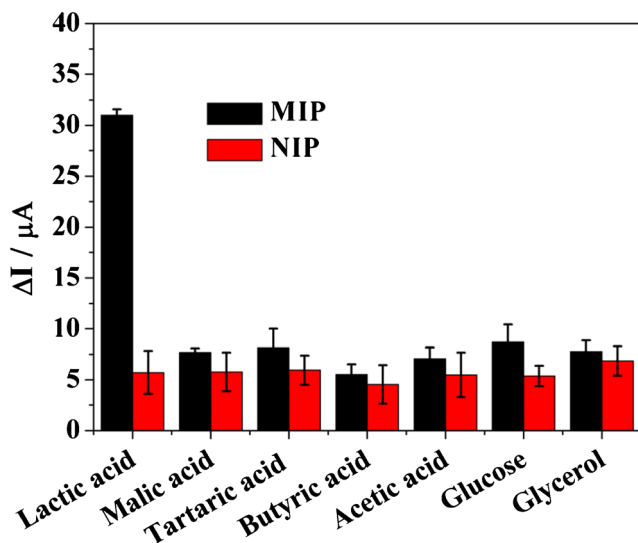$$\beta = \frac{\alpha \, lactic \, acid}{\alpha \, interferent} \quad (3)$$

Fig. 6 Study of interference for the imprinted sensor (MIP) and non-imprinted sensor (NIP). Current response after rebinding of 5.0×10^{-10} mol L^{-1} solution of the interferents under the same conditions used for rebinding of lactic acid

The results obtained are summarized in Table S1. The value obtained for the imprinted factor (α) for lactic acid was found to be relatively higher than that obtained for the interferents; this shows that the imprinted cavities of the sensor exhibit excellent selectivity for analytes detection. The result is confirmed through the analysis of the values of the selectivity factor (β). This behavior suggests that the size and conformation of functional groups in the imprinted cavities were formed specifically to be selective for the detection of lactic acid molecules.

Determination of lactic acid in sugarcane vinasse

The sensor was applied for the determination of lactic acid in sugarcane vinasse samples. The standard addition method, which consists of adding known concentrations of the analyte in the sample, was employed in this investigation. The concentrations of lactic acid applied ranged from 4.0×10^{-10} to 8.0×10^{-10} mol L^{-1}.

The samples were prepared as described in the experimental section. All the measurements were performed in triplicates using different electrodes, and the DPV technique was used to conduct the experiments. The results obtained are presented in Table 2. The lactic acid concentration found was 2.3×10^{-6} mol L$^{-1} \pm 3.1 \times 10^{-7}$ mol L^{-1}.

The average recoveries obtained in this investigation ranged from 97.7% to 104.8% with values for RSD between 2.1 and 4.9%. These results indicate that the method proposed in the study exhibits good accuracy for the determination of lactic acid in sugarcane vinasse; furthermore, the matrix was found to exert no significant effect on the sensor. Based on the data presented, it is strongly believed that the MIP-modified GCE can be successfully applied for the determination of lactic acid in sugarcane vinasse.

Conclusion

A sensor of type MIP/AuNP/RGO/GCE for the determination of lactic acid was obtained by electropolymerization of the o-phenylediamine monomer, on surface modified with reduced graphene oxide (RGO) and gold nanoparticles (AuNPs). The materials used to modify the electrode allowed to obtain low detection limits, limit quantification and good selectivity in the presence of molecules with similar chemical groups and sizes. The recovery values were found to range from 97.7% and 104.8% with *RSD* values between 2.1% to 4.9%. These results show that the method presents good degree of accuracy with no significant matrix effect. The MIP proposed in this work is stable, fast and inexpensive and does not require pre sample preparation. Thus, the sensor proved to be a good alternative for the determination of lactic acid in complex samples.

Compliance with ethical standards

Conflict of interest The authors declare that they have no conflict of interest.

Table 2 Determination of lactic acid in sugarcane vinasse

Sample: Vinasse	Amount added (10^{-10} mol L^{-1})	Amount detected (10^{-10} mol L^{-1})	Recovery (%)	RSD (%)
	4.0	3.9 ± 0,23	97.7	3.7
	6.0	6.2 ± 0,30	104.8	2.1
	8.0	8.1 ± 0,21	102.1	4.9

Concentration of lactic acid 2.3×10^{-6} mol L^{-1}, $\pm 3,1 \times 10^{-7}$ mol L^{-1}

References

1. Andres F, Martinez C, Marcos E et al (2013) Lactic acid properties, applications and production : a review. Trends Food Sci Technol 30: 70–83. https://doi.org/10.1016/j.tifs.2012.11.007
2. Gao C, Ma C, Xu P (2011) Biotechnological routes based on lactic acid production from biomass. Biotechnol Adv 29:930–939. https://doi.org/10.1016/j.biotechadv.2011.07.022
3. Alves R, Oliveira D, Komesu A et al (2018) Challenges and opportunities in lactic acid bioprocess design — from economic to production aspects. Biochem Eng J 133:219–239. https://doi.org/10.1016/j.bej.2018.03.003

4. Vargas E, Ruiz MA, Campuzano S et al (2016) Implementation of a new integrated D -lactic acid biosensor in a semiautomatic FIA system for the simultaneous determination of lactic acid enantiomers. Application to the analysis of beer samples. Talanta 152:147–154. https://doi.org/10.1016/j.talanta.2016.01.063

5. Ismail E, Khaneghah AM, Barba FJ et al (2018) Recent advancements in lactic acid production - a review. Food Res Int 107:763–770. https://doi.org/10.1016/j.foodres.2018.01.001

6. Castro-aguirre E, Iñiguez-franco F, Samsudin H et al (2016) Poly (lactic acid) — mass production , processing , industrial applications , and end of life ☆. Adv Drug Deliv Rev 107:333–366. https://doi.org/10.1016/j.addr.2016.03.010

7. Stre M, Greif G, Sturdík E (2012) A rapid method for determination of L -lactic acid in real samples by amperometric biosensor utilizing nanocomposite. Food Control 23:238–244. https://doi.org/10.1016/j.foodcont.2011.07.021

8. Shimomura T, Sumiya T, Ono M, Itoh T (2012) An electrochemical biosensor for the determination of lactic acid in expiration. Procedia Chem 6:46–51. https://doi.org/10.1016/j.proche.2012.10.129

9. Xiao Y, Li Y, Ying J et al (2015) Determination of alditols by capillary electrophoresis with indirect laser-induced fluorescence detection. Food Chem 174:233–239. https://doi.org/10.1016/j.foodchem.2014.11.046

10. Liang P, Sun M, He P et al (2016) Determination of carbohydrates in honey and milk by capillary electrophoresis in combination with graphene – cobalt microsphere hybrid paste electrodes. Food Chem 190:64–70. https://doi.org/10.1016/j.foodchem.2015.05.059

11. Molnar-Perl I (1999) Simultaneous quantitation of acids and sugars by chromatography : gas or high-performance liquid chromatography ? J Chromatogr A 845:181–195

12. Medeiros PM, Simoneit BRT (2007) Analysis of sugars in environmental samples by gas chromatography – mass spectrometry. J Chromatogr A 1141:271–278. https://doi.org/10.1016/j.chroma.2006.12.017

13. Casella IG, Gatta M, Desimoni E (1998) Applications of a copper-modified gold electrode for amperometric detection of polar aliphatic compounds by anion-exchange chromatography. J Chromatogr A 814:63–70

14. Hanko VP, Rohrer JS (2000) Determination of carbohydrates, sugar alcohols, and glycols in cell cultures and fermentation broths using high-performance anion-exchange chromatography with pulsed Amperometric detection. Anal Biochem 283(199):192–199. https://doi.org/10.1006/abio.2000.4653

15. Cm M, Sk A, Fleming SC et al (1990) Rapid and simultaneous determination of lactulose and mannitol in urine , by HPLC pulsed Amperometric detection , for use in studies of intestinal permeability with. Clin Chem 36:797–799

16. Kim S, Kim K, Kim H et al (2018) Non-enzymatic electrochemical lactate sensing by NiO and Ni (OH) 2 electrodes : a mechanistic investigation. Electrochim Acta 276:240–246. https://doi.org/10.1016/j.electacta.2018.04.172

17. Ibupoto ZH, Muhammad S, Ali U et al (2012) Electrochemical L-lactic acid sensor based on immobilized ZnO Nanorods with lactate oxidase. Sensors 12:2456–2466. https://doi.org/10.3390/s120302456

18. Mazzei F, Botrè F, Favero G (2007) Peroxidase based biosensors for the selective determination of D, L-lactic acid and L-malic acid in wines. Microchem J 87:81–86. https://doi.org/10.1016/j.microc.2007.05.009

19. Pariente F, Lorenzo E (2006) Design and characterization of a lactate biosensor based on immobilized lactate oxidase onto gold surfaces. Anal Chim Acta 555:308–315. https://doi.org/10.1016/j.aca.2005.09.025

20. Gamero M, Pariente F, Lorenzo E, Alonso C (2010) Biosensors and bioelectronics nanostructured rough gold electrodes for the development of lactate oxidase-based biosensors. Biosens Bioelectron 25:2038–2044. https://doi.org/10.1016/j.bios.2010.01.032

21. Romero MR, Garay F, Baruzzi AM (2008) Design and optimization of a lactate amperometric biosensor based on lactate oxidase cross-linked with polymeric matrixes. Sensors Actuators B Chem 131:590–595. https://doi.org/10.1016/j.snb.2007.12.044

22. Suman S, Singhal R, Sharma AL et al (2005) Development of a lactate biosensor based on conducting copolymer bound lactate oxidase. Sensors Actuators B Chem 107:768–772. https://doi.org/10.1016/j.snb.2004.12.016

23. Chen L, Wang X, Lu W, Wu X, Li J (2016) As featured in: molecular imprinting: perspectives and applications. Chem Soc Rev 45:2137–2211. https://doi.org/10.1039/C6CS00061D

24. Sharma PS, Pietrzyk-le A (2012) Electrochemically synthesized polymers in molecular imprinting for chemical sensing. Anal Bioanal Chem 402:3177–3204. https://doi.org/10.1007/s00216-011-5696-6

25. Malitesta C (1827–1846) Mazzotta E (2012) MIP sensors – the electrochemical approach. Anal Bioanal Chem. https://doi.org/10.1007/s00216-011-5405-5

26. Vanossi D, Pigani L, Seeber R et al (2013) Electropolymerization of ortho-phenylenediamine. Structural characterisation of the resulting polymer film and its interfacial capacitive behaviour. J Electroanal Chem 710:22–28. https://doi.org/10.1016/j.jelechem.2013.04.028

27. Alizadeh T, Nayeri S, Mirzaee S (2019) A high performance potentiometric sensor for lactic acid determination based on molecularly imprinted polymer / MWCNTs / PVC nanocomposite fi lm covered carbon rod electrode. Talanta 192:103–111. https://doi.org/10.1016/j.talanta.2018.08.027

28. Luiz J, Beluomini MA, Sedenho GC, Stradiotto NR (2017) Determination of amino acids in sugarcane vinasse by ion chromatographic using nickel nanoparticles on reduced graphene oxide modi fi ed electrode ☆. Microchem J 134:374–382

29. Beluomini MA, Silva JL, Sedenho GC, Stradiotto NR (2017) D -mannitol sensor based on molecularly imprinted polymer on electrode modi fi ed with reduced graphene oxide decorated with gold nanoparticles. Talanta 165:231–239. https://doi.org/10.1016/j.talanta.2016.12.040

30. Ariffin AA, O'Neill RD, Yahya MZA, Zain ZM (2012) Electropolymerization of ortho-phenylenediamine and its use for detection on hydrogen peroxide and ascorbic acid by electrochemical impedance spectroscopy. Int J Electrochem Sci 7:10154–10163

31. Fall M, Diagne AA, Dieng MM et al (2005) Electrochemical impedance spectroscopy of poly(3-methoxythiophene) thin films in aqueous LiClO4 solutions. Synth Met 155:569–575. https://doi.org/10.1016/j.synthmet.2005.09.043

32. Karimian N, Vagin M, Hossein M et al (2013) Biosensors and bioelectronics an ultrasensitive molecularly-imprinted human cardiac troponin sensor. Biosens Bioelectron 50:492–498. https://doi.org/10.1016/j.bios.2013.07.013

33. Kor K, Zarei K (2016) Development and characterization of an electrochemical sensor for furosemide detection based on electropolymerized molecularly imprinted polymer. Talanta 146:181–187. https://doi.org/10.1016/j.talanta.2015.08.042